Analytical Design of a Vernier Variable Reluctance Machine with Smooth Exited Rotor

A. Dekhinet*, S. Taïbi*, A. Tounzi**
* Department of Electrical Engineering, Batna University, ABDEKHINET@yahoo.fr
** Laboratoire d'Electrotechnique et d'Electronique de Puissance de Lille.

Abstract – *In the field of energy conversion applications, the tendency of electrical machine design directly coupled is being directed towards those capable of operating at low speed and high torque. The Vernier variable reluctance machines (VVRM) can meet these requirements.*
In this paper, we introduce the Vernier effect principle and interest on the basis of the air gap energy assessment, and suggest therefore, a detailed sizing method that leads to a prototype of VVRM with smooth excited rotor. A set of results of this prototype are included.
In order to validate the adopted analytical design procedure, the prototype results are compared to numerical ones obtained from a finite elements analysis.

Keywords – *Electric Machines, Variable reluctance machine (VRM), Design, Vernier machine, direct driven.*

I. INTRODUCTION

Since several years, a considerable interest has been focused on direct driven structures, [1-4] to be used for applications requiring low speed and high torque. This operation can be ensured by either permanent magnet synchronous machines with high pair pole number [5] or by variable reluctance machines [6]. The structures can be discoid or cylindrical [7]. Most of the papers that deal with these particular structures do not give the sizing procedure which leads to their prototypes.

The purpose of this paper is to present a design procedure that yields a primary structure. The proposed structure is a Vernier variable reluctance type machine excited by windings supplied by an AC balanced polyphase current or by a DC current.

The electrical machine design is based on two considerations. The first one is the geometric design of the two frames (rotor and stator). The second concerns the design of the electrical circuits (windings) and their power supply.

In general, the overall dimensions of the electrical circuit depend on the *m.m.f.* required for the magnetic field production, directly linked to the desired power.

The magnetic circuit sizing should take into account its ability to canalize the magnetic field while limiting a decrease of the magnetic potential difference. This design will therefore depend directly on the magnitude of the created field.

In the first part of this paper, we introduce the operation principle of the VVRM to highlight the Vernier effect interest.

The second part is devoted to the conditions to be met to ensure a proper operating of excited smooth rotor Vernier variable reluctance machine. For this aim, an analytical model based on the magnetic energy is introduced and the conditions on the stator teeth and pair pole numbers are deduced

Then, a procedure to design a prototype of such structure is introduced. The different design stages conducting to a primary prototype are given and explained.

At last, using the sizing procedure, a prototype has been designed. We studied it using 2D-FEM analysis. The results are compared to the ones obtained from the analytical sizing procedure.

II. VERNIER VRM OPERATING PRINCIPLE

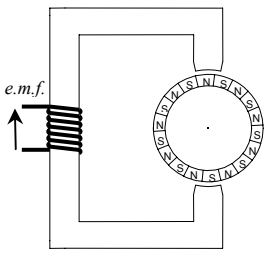

Fig 1.

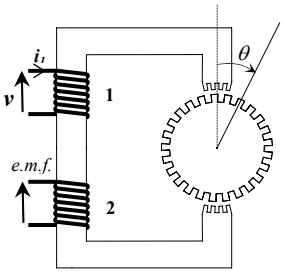

Fig 2.

Fig. 1. Permanent magnet classical structure

Fig. 2. Double teeth excited stator structure with Vernier effect.

In order to explain the operating principle of an excited vernier machine and its interest, two structures are introduced. The first one is constituted

of a polar wheel with p pairs of poles and a ferromagnetic yoke supporting a winding Fig. 1. When the wheel is driven at a speed Ω, an *e.m.f*, of pulsation ω, is induced in the coil surrounding the yoke. This pulsation is directly proportional to the product $p\Omega$. In the case of low speed, the pulsation is low as well. Therefore, in order to obtain an *e.m.f.* of significant frequency while rotating at low speed, it is necessary to increase the number of the pole pairs.

The second structure depicted in Fig. 2 is constituted of a ferromagnetic yoke with N_s teeth and a wheel of N_r teeth. Furthermore, two separate windings are wound around the yoke. The first one, referred as the excitation circuit, is carrying a DC or AC current i_1 which ensures the circuit magnetisation. The second one, referred as the armature circuit, will collect the induced *e.m.f.* Let θ represents the reference axis position of the rotor with respects to the stator reference axis. The total air gap reluctance that depends on rotor position can be expressed as $R(\theta)$.

Let us consider a generator operating, i.e. the wheel is rotated and the excitation circuit is energized. If i_1 is a DC current, for the same rotational speed Ω, the *e.m.f.* induced in the armature winding will have a frequency that will be much higher than the case presented in Fig. 1. It will be mainly a function of the air gap reluctance periodicity.

If i_1 is a sinusoidal current of a frequency f_1, the frequency f_2 of the induced *e.m.f.* will depend on Ω, air gap reluctance periodicity and f_1. It is therefore possible, for a given speed and desired frequency f_2, to supply a current i_1 with an adequate frequency f_1.

The excitation circuit can be moved from the stator in order to be located in the rotor. Thus, we obtain the structure shown in Fig. 3. This operates in the same manner as the structure seen in Fig. 2. with an additional degree of freedom that is the rotor position θ.

In order to maximize the active surface while keeping the Vernier effect, it is possible to suppress the saliency of one of both surfaces. Hence, in the case of an smooth rotor solution, we yield the structure shown in Fig. 4

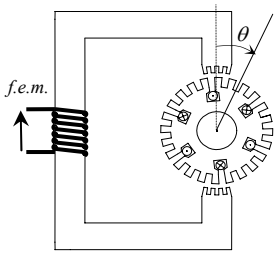

Fig. 3.

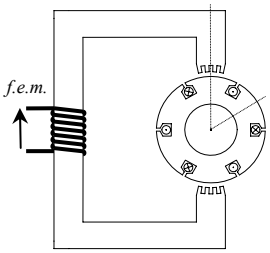

Fig. 4.

Fig. 3. Double teeth excited rotor structure with Vernier effect.
Fig. 4. Smooth excited rotor structure with Vernier effect

For the proper functioning of the structure we must combine correctly between the operating parameters of the MRVV: N_r, N_s, p, p' and Ω. This point will be the subject of the following section.

III. ENERGY MODEL AND OPERATING CONDITIONS OF A SMOOTH ROTOR VVRM

To determine the combination between the stator teeth and the polarities of both excitation and armature circuits to reach a synchronous operating, we use the structure presented in Fig. 5 which is a generic cylindrical of a current rotor excited stator teethed reluctance machine.

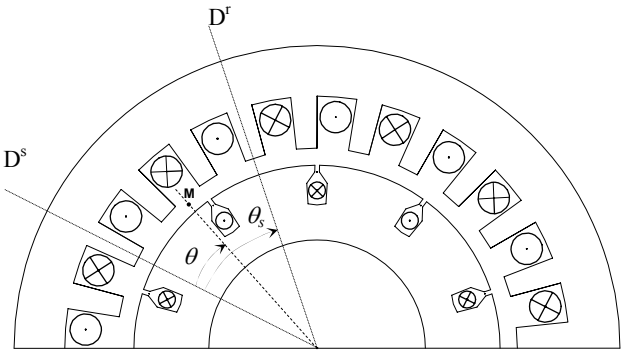

Fig. 5: Cylindrical structure of a current rotor excited stator teethed reluctance machine

To yield theses conditions, as well as the relation between the frequencies and the rotation speed, we introduce an analytical model of the magnetic energy in the system. This model is based on the hypothesis of an infinite magnetic permeability of the iron. Therefore, the magnetic energy is limited to the one stored in the air gap.

1- Energy expression

The expression of the total energy W_{em} in the air gap of an excited Vernier reluctance machine can be expressed by the following relation :

$$W_{em} = \frac{1}{2}\int_0^{2\pi} \mathcal{E}_e^2(\theta_s,\theta)\ P(\theta_s,\theta) \quad d\theta_s \qquad (1)$$

where ε is the magneto motive force in the air gap and P represents the air gap permeance. θ_s is the position of a given point M in the air gap with respect to the stator frame and θ the angle between the rotor and the stator frames.

2- Air gap permeance

The air gap permeance, per angle unit, depends mainly on the geometric parameters related to the structure. In the case of a smooth rotor VVRM, this permeance can be written, as follows [1], :

$$P(\theta_s,\theta) = \mu_0 L\ R_s E_0 + \sum_{j=1}^{\infty} \mu_0 L\ R_s E_s e_j \cos(j N_s \theta_s) \qquad (2)$$
$$= P_0 + P_s(\theta_s)$$

P_0 represents a constant term related to the average air gap width value and $P_s(\theta_s)$ is function of the stator saliency. E_0, Es and e_j are geometric coefficients .

3-Difference of air gap magnetic potential

As the permeability of the iron is assumed to be infinite, we consider a radial field distribution in the air gap. In this case, when a winding k creates an *m.m.f.* its expression can be written in a series form as:

$$\varepsilon_k = \sum_{i=0}^{\infty} \frac{2}{\pi}\frac{n_k \cdot i_k}{(2i+1)} \sin((2i+1)\frac{\pi}{2}) K_{Bk}^i \cos\left((2i+1) p_k \theta_s\right) \qquad (3)$$

A q phase circuit, located in the same armature, creates a *m.m.f.* that the resulting expression, is obtained by the algebraic sum of the *m.m.f.* of each phase. Thus, the armature winding embedded in the stator, gives a total *m.m.f* ε_T expressed as:

$$\varepsilon_T = \sum_{i=0}^{\infty} [\frac{q}{2}.\frac{2}{\pi}.\frac{n.I_{max}}{(2i+1)} \sin((2i+1)\frac{\pi}{2}) K_B^i].\cos\left(\omega t - (2i+1).p\theta_s\right) \qquad (4)$$

The inductor windings, driven by the rotor, give a total *m.m.f* given by:

$$\mathcal{E}'_T = \sum_{i=0}^{\infty} [\frac{q'}{2}\frac{2}{\pi}\frac{n'\ I'_{max}}{(2i+1)} \sin((2i+1)\frac{\pi}{2})\ K_B^i] \cos\left(\omega t - (2i+1)\ p'\ (\theta_s - \theta)\right) \qquad (5)$$

4- Energy and conditions of conversion

To ensure the conversion of the electrical energy, it is necessary that the structure develops a rotating torque. This implies that the magnetic energy in the air gap must be a function of the rotor position θ. Now, the expression of this energy (1) involves the air gap permeance which is essentially a function of the stator teeth numbers N_s. It involves also the term that expresses the total *m.m.f* due to the winding supplies. In this term, it the polarities p and p' appear.

These conditions are related to the number of teeth of the stator and the polarity of the two circuits: power and excitation supplies. They are based on the fact that the smooth VVRM structure must produce an electromagnetic torque with an average value non-zero [9-11]. Furthermore, the torque has to present minimal ripples. Therefore, the structure will only use the main electromagnetic conversion that corresponds to the interaction between the armature and excitation fields through the variation of the air gap permeance.

In the case of smooth rotor VVRM, these conditions are expressed by the following relations:

$$\begin{cases} \pm N_s = \pm p \pm p' \\ p \neq p' \\ N_s \neq 2p \\ N_s \neq 2p' \end{cases} \qquad (6)$$

Then, the magnitude of the main electromagnetic torque is given by:

$$T_e = \frac{9}{\pi} p'\ n\ n'\ I\ I' K_B K_B' P_s \qquad (7)$$

This torque is constant when the rotor rotates at the following synchronous speed:

$$\Omega = \frac{\pm\omega \pm \omega'}{p'} \qquad (8)$$

IV. SIZING PROCEDURE

The dimensioning of electrical machines requires preliminary data which represent mainly the features of the nominal operating: The output power and the power factor, the supply voltage magnitude and its frequency and the rotating speed.

The design of an electrical machine is based on two considerations. The first one is related to the geometric dimensioning, in other words, the magnetic circuits of the rotor and stator, as well as the slots of both armatures. The second consideration is the design of the electrical circuit, thus the distribution of windings on both armatures and their supply. These two parts are imbricated. Globally, the dimensions of the electrical circuit depend on the ampere-turns required for the production of the magnetic field, directly linked to the desired power.

The dimensions of the magnetic circuit should take into account its ability to canalize the magnetic field by limiting the magnetic potential difference drops. This design will therefore depend directly on the magnitude of the field which should be canalized.

1- Determination of the D^2L magnitude

The useful volume of a structure is defined by the value of the variable D^2L, which is expressed, in function of the apparent power S, by the following relation:

$$S = \frac{\pi^2}{60\sqrt{2}} N (K_B / K_f) K_S D^2 L \; B_e A_c \qquad (9)$$

The various parameters of this relation are specified in the nomenclature at the end of the paper.

To separate the internal diameter D from the effective length L, one of the two parameter sizes has to be chosen. This choice is made further to a number of constraints. These constraints can affect bulkiness, linear speed or the optimal use of copper.

In order to increase the air gap permeance, and hence the electromagnetic energy, it is advantageous to choose the lowest possible minimum air gap. This choice depends on constraints related to the mechanical implementation. For the studied structure, the minimum air gap is taken equal to 0.3 mm. Actually, this size is easily achievable, for a internal diameter of about 0.5 m [1].

2- Design of VVRM slots and yokes

From a geometric point of view, it remains to determine the seven parameters ($l_{er}, l_{ds}, l_{es}, p_{ys}, p_{yr}, p_r$ and p_s) defined in the Fig. 6

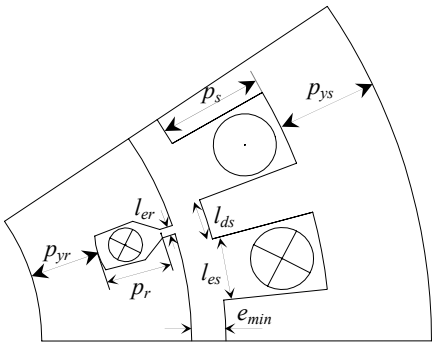

Fig. 6: Identification of geometric parameters

The first step, in the design of slots, is to choose the stator tooth width l_{ds} according to the tooth step $\lambda_s = l_{ds} + l_{es}$. The electromagnetic torque ripple in a VVRM structure is very sensitive to this tooth width [5]. To limit the torque ripple, the ratio $r_{ds} = l_{ds} / \lambda_s$ should be included in the interval [0.4, 0.5] [1].

The calculation of the ampere-turns in a slot, for the maximal operating mode ($AT_{\max/slot}$), allows us to determine the depth of the stator and the rotor slots. The stator slot depth is given by:

$$p_s = \frac{AT_{\max/\,slot\ stator}}{D_c K_{rem} l_{es}} \qquad (10)$$

Where D_c is the current density and K_{rem} represents the fill factor. The same formula, with the rotor parameters, can be applied to calculate its slot depth p_r.

In order to attenuate the saturation effects, we choose the thickness of the rotor and stator cylindrical yokes, noted p_{ys} and p_{yr} respectively, function of the widths of the stator tooth. These values can be obtained as follows:

$$\begin{cases} p_{ys} \geq sup\,(q_e\,, q'_e)\, l_{ds} / 2 \\ p_{yr} \approx p_{ys} \end{cases} \qquad (11)$$

3- Design of the windings

In the studied structure, the excitation circuit is made up of windings. The calculation of the excitation ampere-turns is deduced from the rated operating point. The calculation of the ampere-turns requires the knowledge of the rated armature winding and inductor currents, and the turn number in each winding, such as:

$$AT_{\max/enc\ sta} = \sqrt{2}\left(\frac{n}{q_e} I\right) \tag{12}$$

Other parameters, which are the number of turns of the armature and the excitation windings, are obtained from two relations. The first one is based on the flux expression per phase and the second one on the equality of the ampere-turns between inductor and armature winding.

The flux linkage in an armature winding phase is expressed as a function of the excitation *m.m.f.* and the air gap permeance, as given below:

$$\phi_k = \int_0^{2\pi} \varepsilon'_T\ F_k\ P(\theta_s,\theta)\quad d\theta_s \tag{13}$$

In this expression, the term F_k represents a filter function permitting to isolate the phase *k* of the armature winding circuit. This function constitutes the *k* winding distribution and can be written, taking into account the only first terms, under the following form:

$$F_k = \frac{2}{\pi} K_B\ n \cos\left(p\theta_s - (k-1)\frac{2\pi}{3}\right) \tag{14}$$

Where *k* = 1, 2 or 3 is the order of the considered phase.

Replacing (14) into the relation (13), the flux linkage in an armature winding phase, when the machine is running at the synchronous speed, can be expressed as:

$$\phi_k = \frac{3}{\pi} K_B\ K'_B\ n\ n' I' P_{1s} \cos\left(\omega t - (k-1)\frac{2\pi}{3}\right) \tag{15}$$

Starting from the desired value of the *e.m.f.* $e_k = -d\phi_k / dt$ and the choice of excitation current *I'*, we obtain a value for the product *n n'*.

In order to optimize the energy conversion of the machine, the ampere-turns of the armature winding and the inductor circuits have to be equal [1]. In such circumstances, we can write :

$$p K_B\ n\ I = p' K'_B\ n' I' \tag{16}$$

This last expression combined with the product value of nn' permits to determine the number of turns of both stator and rotor circuits.

4- Expressions of self and mutual inductances

The self inductance of phase *k* can be obtained by calculating the flux linkage through this phase when it is fed by a unit DC current. The mutual inductances are determined in the same manner, by calculating the flux throughout the other phases.

Consequently, the self and mutual inductances can be expressed by:

$$L_{lm(m=l)} = \int_0^{2\pi} \varepsilon_l\ F_m\ P(\theta_s,\theta)\quad d\theta_s \tag{17}$$

$$M_{lm(m\neq l)} = \int_0^{2\pi} \varepsilon_l\ F_m\ P(\theta_s,\theta)\quad d\theta_s \tag{18}$$

Where the index *l* is the phase winding in which the unit current is imposed. The index *m* is related to the phase in which the flux linkage is calculated. The *m.m.f.* ε_l, is obtained from the general expression of the *m.m.f.* given by the relation (3). These expressions give:

$$L_{11} = \frac{4}{\pi} n^2\ K_B^2\ P_0\ ; \qquad L_{44} = \frac{4}{\pi} n'^2\ K'^2_B\ P_0 \tag{19}$$

$$M_{14} = \frac{2}{\pi} P_{1S}\ K_B K'_B\ n\ n' \cos(p'\ \theta) \tag{20}$$

V. DESIGNED PROTOTYPE

A prototype has been designed using the sizing procedure developed above. Its specifications are given in the following table:

Table 1: Prototype specifications

Active power	Voltage	Power factor	Rotation speed
P=5 KW	V=220 V	0.8	N=50 rpm

In Fig. 7, we give the geometrical characteristics of the designed prototype.

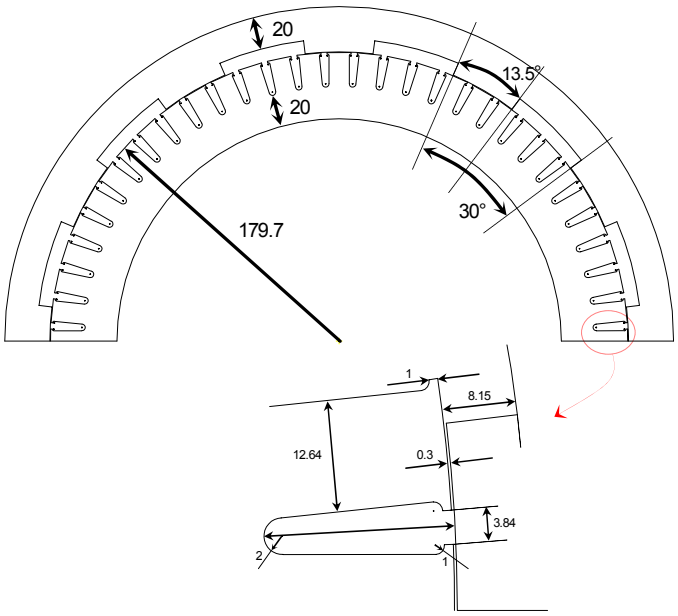

Fig. 7: Geometrical parameters of the designed prototype

Table 2: Characteristics of the designed prototype

VVRM-Prototype		$p=2$	$p'=10$	$N_s=12$	$\Omega=5.23$ rad/s
$n=130$		$n'=82$	$q_e=1$	$q'_e=1$	$f'=58$ Hz
$I=9A$	$I'=2.8A$	$L=270$	$q=3$	$q'=3$	$f=50$ Hz

In the sake of validating the operating principle and the sizing procedure developed previously, we used the finite element method to perform accurate analysis. A comparison of results such as self inductances, mutual inductances and the *e.m.f.* at no load between the analytical and finite element models is presented. The finite element calculations, taking into account the movement, is fulfilled with the calculation code developed in the laboratory L2EP of Lille (France).

In Fig. 8, we present the 2D mesh in a cutting plane of the prototype. It is constituted of 39500 elements and 19900 nodes.

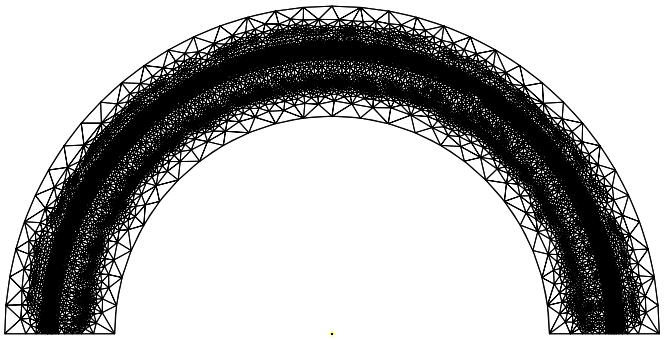

Fig. 8: Mesh in a cutting plane of the prototype

The field distribution in a cutting plane of the structure, at no load, is presented hereafter. One can clearly notice the excitation poles modulated by the permeance air gap. Only two poles seem to be energized on half part of the structure. This corresponds to the difference between the armature and the excitation pole pair numbers.

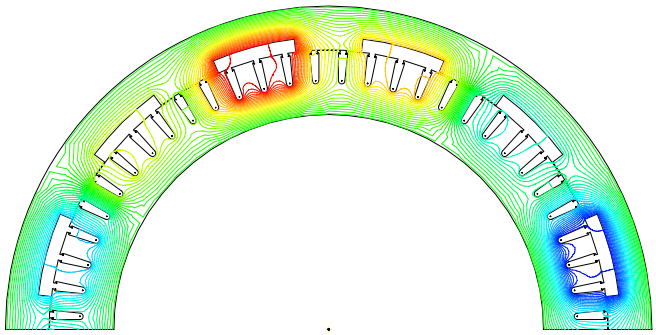

Fig. 9: Field distribution, at no load, in a cutting plane of the structure

Calculations have been carried out at no load. In the case of the self inductances presented in the Fig. 10 and 11, numerical computations show slight ripples. This does not appear on the analytical calculation because it does not take into account the small slots in the rotor.

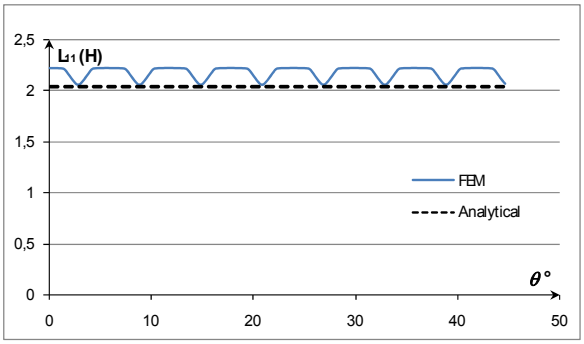

Fig. 10: The self inductance of an armature phase winding

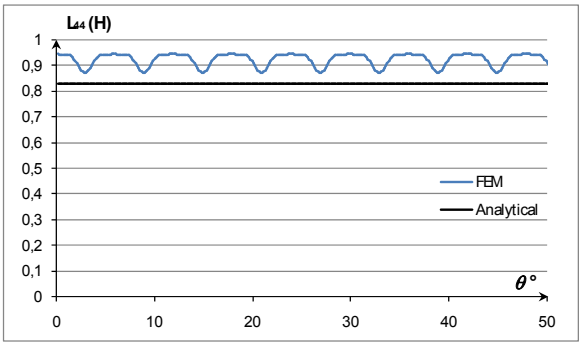

Fig. 11: The self inductance of an excitation phase winding

In Fig. 12, we present a mutual inductance between the armature and excitation windings. As expected, it has a sinusoidal waveform. We also note that the frequency of this wave, equal to $p'\Omega/2\pi$, corresponds exactly to that found analytically in the equation (20).

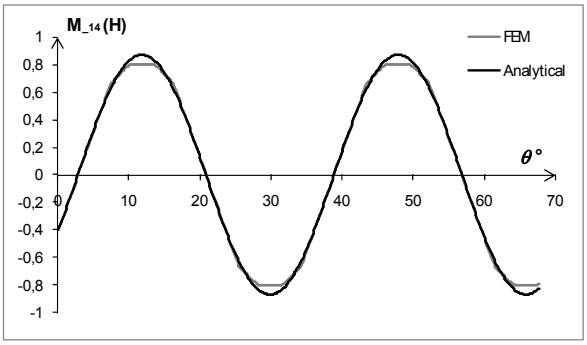

Fig. 12: Mutual inductance between armature and excitation windings

Using 2D-FEM code, we calculate the no load flux when the excitation circuit is supplied at the rated frequency and the rotor rotates at the synchronous speed. In Fig. 13, we present a no load linkage flux. It has a sinusoidal waveform with a magnitude that corresponds to the no load *e.m.f.* imposed during sizing procedure. Furthermore, the frequency is equal to 50Hz and meets our expectations.

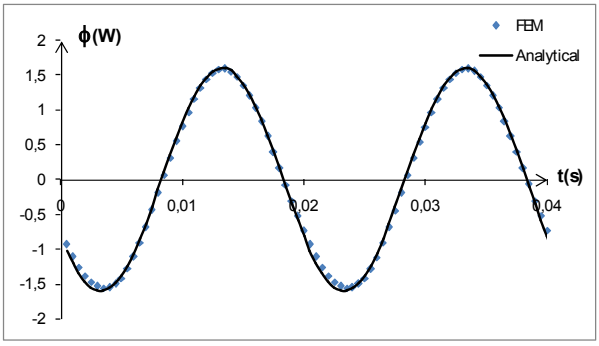

Fig. 13: No load flux per phase at I'=0.85 A

Finally, we show, in Fig.14, the no load torque of the designed prototype obtained from numerical calculations. The ripples of this torque are relatively high related to the rated torque. Indeed, the rotor slots induced an additional variable reluctance that leads to an electromagnetic conversion whose synchronous speed is different from the one of the main conversion.

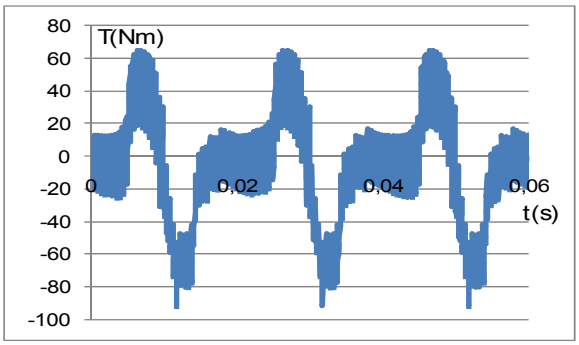

Fig. 14: No load torque of the designed prototype at I'=2.8.

In order to decrease the magnitude of these ripples, it is possible to skew the slots of the rotor by an angle equal to the stator tooth step. Using the slice technique coupled to 2D-FEM, we carried out calculations to simulate the no load operating with skewed rotor slots.

In Fig.15, we show the results obtained with 10 slides. We can notice that the magnitude of the torque ripples is divided by 2.

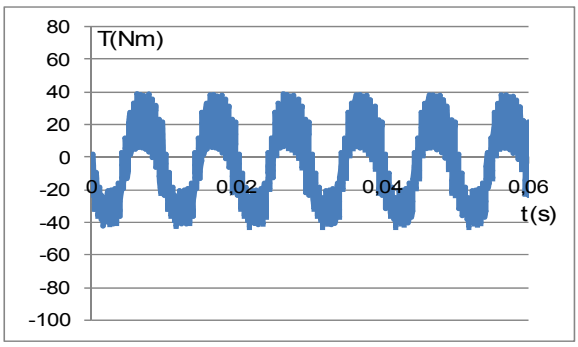

Fig. 15: No load Torque at I'=2.8 A with virtual tilt rotor teeth.

Calculations have also been performed at load using 2D-FEM. In this case, the excitation circuit is supplied by its rated currents while the armature windings are supplied by half the rated magnitude. Besides, the rotor is moved at its rated synchronous speed. In the following table, we give the average values of the electromagnetic torque. We compare the analytical value to the ones obtained by the numerical model at linear and non linear iron characteristic.

Table 3: Average values of the electromagnetic torque

Analytical model	2D-FEM linear case	2D-FEM non linear case
492 Nm	454 Nm	200 Nm

We can notice that the value obtained by the 2D-FEM when the magnetic material is supposed with a linear behavior is close to the one calculated by the analytical model. This validates, in a first attempt, the design procedure introduced. When we take into account the non linearity of the magnetic material, the average value is divided by a ratio greater than 2. This confirms the high saturation level of such structures and the necessity to use numerical models, as FEM, to optimize the design of the structure.

CONCLUSION

In the first part of this work, we introduced an energy model based on the air gap permeance and *m.m.f.*, for rotor excited vernier variable reluctance machines with a smooth rotor. This model has allowed us to determine the conditions on the teeth and the polarities of windings to ensure a synchronous operating of these machines.

In the second part, we established a sizing procedure, which allows leading to a detailed plan of an initial machine structure.

To validate the proposed sizing procedure, a comparison between the results of the proposed model and a 2D-FEM analysis is presented.

The obtained results, in the hypothesis of an infinite magnetic permeability of the iron, correspond to the expected ones and are very similar for both models. These validate the principle of the studied structure and the proposed pre-sizing procedure.

X. NOMENCLATURE

N_s: Stator teeth Number
P: Number of pairs of poles of the armature winding
P': Number of pairs of poles of the inductor coils
B_e : Air gap magnetic induction
θ : Rotor position with respect to stator axis
θ_s : Air gap position with respect to stator axis
L : Machine effective length
R_s : Internal radius
$K_{Bk}^{\ i}$: Coefficient of windings for the ith harmonic
K_B : Fill factor of the armature winding
K'_B : Fill factor of the inductor winding
i_k : Supply current of the winding k
I_{max} : Supply maximum current
I'_{max} : Maximum excitation current
I : Supply r.m.s Current food
I' : Excitation r.m.s Current
ω : Pulsation of the armature winding currents
ω' : Pulsation of the inductor currents
n : Number of turns of the armature winding
n' : Number of turns of the inductor winding
q : Number of phases of the armature winding
q' : Number of phases of the inductor winding
q_e : Number of slots by sector and by armature winding phase
q_e' : Number of slots by sector and by phase of the inductor
A_c : Linear current density
K_f : Coefficient of flux waveform
K_S : Coefficient of active surface in the air gap
N : The rotation speed in rpm

XI. REFERENCES

[1] S. Taibi, A. Tounzi, F. Piriou. "Study of stator current excited Vernier reluctance machine " IEEE Transactions on Energy conversion, Vol. 21, 2006, pp : 823-831

[2] H. Murakami & ALL " Optimum Design of Highly Efficient Magnet Assisted Reluctance Motor " IEEE Industry applications conference, Vol. 4, 2001, pp: 2296-2301

[3] A. Boglietti, A. Cavagnino, M. Pastorelli, A. Vagati " Experimental Comparison of Induction and Synchronous Reluctance Motors Performance " IEEE Industry applications conference, Vol. 1, 2005, pp : 474-479.

[4] P. Lampola, J. Vânâen, "Analysis of a low speed permanent-magnet wind generator connected to a frequency converter ", ICEM 96, vol. 2, pp: 393-398.

[5] L. Söderlund, T.T. Eriksson, J. Salonen, H. Vihriälä, R. Perälä, " A permanent-magnet generator for wind power applications" IEEE Trans. on Magnetics, vol. 32, n°4, 1996.

[6] D.J. Rhodes "Assessment of Vernier motor design using generalised machine concepts" IEEE Transactions on Power Apparatus and Systems, Vol. PAS-96, n°4, 1977

[7] I. Haouara, A. Tounzi, F. Piriou "Design and optimisation of an excited reluctance generator using field computation"IEEE Trans. Mag., Septembre 1998, pp.3494-3497.

[8] A. Toba, T. A. Lipo "Generic Torque-Maximizing Design Methodology of Surface Permanent-Magnet Vernier Machine" IEEE Trans Ind. Appl, vol 36, n°6, Nov 2000, pp:1539-1546.